25^{th} EUROPEAN ROTORCRAFT FORUM

Paper H1

Effect of Drive Train and Fuel Control Design on Helicopter Handling Qualities

Giorgio Guglieri

Politecnico di Torino
Dipartimento di Ingegneria Aeronautica e Spaziale
Torino - Italy

September 14-16, 1999
Rome - Italy

ASSOCIAZIONE INDUSTRIE PER L'AEROSPAZIO, I SISTEMI E LA DIFESA
ASSOCIAZIONE ITALIANA DI AERONAUTICA ED ASTRONAUTICA

Effect of Drive Train and Fuel Control Design on Helicopter Handling Qualities

Giorgio Guglieri *
Politecnico di Torino
Dipartimento di Ingegneria Aeronautica e Spaziale
Corso Duca degli Abruzzi, 24
10129 - Torino (Italy)

Abstract

A comprehensive formulation for drive train torsional dynamics is included in a high order mathematical model. The dynamic response is validated for a realistic helicopter configuration. The effects of governor and drive train design parameters on rotorcraft stability in hovering flight are analyzed. Two different mathematical models are considered: a high order blade element type model (34 DOFs) and a reduced order analytical model (8 DOFs). The impact of rpm-governor design parameters on the application of some relevant ADS-33D handling qualities criteria is also evaluated.

Nomenclature

c_ζ	Lag damper coefficient
e	Hinge offset
k_ζ	Lag damper coefficient
K_D	Fuel controller derivative gain
K_P	Fuel controller proportional gain
K_I	Fuel controller integral gain
K_C	Collective anticipation gain
I_{eq}	Equivalent inertia
I_ζ	Blade moment of inertia
M_ζ	Blade mass moment
m_ζ	Blade mass
n_b	Number of blades
Q	Shaft torque ($Q = r_g Q_E$)
Q_E	Engine torque
r_g	Engine to rotor rpm ratio
TPI	Politecnico di Torino
T_Q	Torque dynamics derivative
T_{wf}	Torque dynamics derivative
$\mathbf{x}$	State vector
$\mathbf{u}$	Control vector
w_f	Governor fuel flow rate
β	Flap angle of main rotor blade
ζ	Lag angle of main rotor blade
μ	Advance ratio
θ_o	Collective pitch of main rotor
θ_{1s}, θ_{1c}	Cyclic pitch components
θ_{TR}	Collective pitch of tail rotor
ψ_b	Rotor hub angular displacement
ψ_1	Shaft angular displacement at the exit of the gearbox
τ_{wf}	Fuel flow time constant
ξ	Damping ratio
ω_n	Natural frequency
Ω	Main rotor angular velocity ($\Omega = \dot{\psi}_b$)
Ω_1	Shaft angular velocity ($\Omega_1 = \dot{\psi}_1$)

*Assistant Professor, Member AIAA-AHS

Presented at the 25th European Rotorcraft Forum, Rome, Italy, September 14-16, 1999

Introduction

Large rpm variations may produce a significant degradation of aircraft handling qualities in maneuvering flight [4, 5]. The trend towards using lower inertia rotor systems in modern helicopters reduces the level of kinetic energy stored in the system and makes the rotor more susceptible to large variations in its rotational speed during rapid maneuvers.

Severe torsional oscillations in the helicopter rotor drive shaft, and dynamic interface problems involving rotor, drive train and airframe subsystems were also observed in several testing conditions [11]. The interaction of rotor, engine and control on the CH-47C helicopter resulted in unacceptable torque and fuel flow oscillation in early flight test aircraft. Based on a flight test program [6], fuel control gains and time constant changes were suggested (reduced gain and "slowed down" fuel control). It was also observed that blade lag dampers may actually raise the natural frequency of the important turbine-rotor torsional mode due to the compressibility spring effect. A correlation between torsional instability and damper preload force level was also found.

A complete review of rotor / engine dynamics problems is presented in Refs. [11, 13, 14].

A time domain analysis of coupled engine / drive train / rotor dynamics of a twin-engine, single main rotor helicopter model is performed in Ref. [11]. The analysis incorporates an existing helicopter model with nonlinear simulations of a turboshaft engine and its fuel controller. A linearized four state engine model is shown to reasonably predict engine states and outputs, shortly after the control input. Sensitivity of rotor rpm droop to fuel controller gain changes and collective input feed-forward gain changes are studied. For the rotor and propulsion system modeled, rotor inplane dynamics is not significantly affected by drive train dynamics. It was found that retaining the collective pitch feed-forward path in the fuel controller improved main rotor rpm and power turbine engine speed governing characteristics. The load sharing between the two engines is shown to result in lightly damped rotor inplane oscillations, directly excited by the low frequency dynamics in one engine's torque.

The increase in the responsiveness of the engine / fuel control system using a conventional rotor speed governor can severely compromise the stability margin of the torsional dynamics of the rotor system [13]. The possible proposed solutions are: either the decoupling of control laws between engine fuel control and airframe / rotor dynamics or the integration of power management into the flight control system. The emergence of digital engine controls and the parallel development of digital flight controls make possible the application of a fully integrated digital flight/propulsion control system.

Much of the industry experience with rotor / engine dynamics problems is reported in Ref. [14]: (i) excessive rotor induced vibration of the propulsion system (ii) excessive vibration (forced or self-excited) because of engine / drive train / rotor resonances (iii) engine / drive train torque oscillations, often involving high gain fuel control systems (iv) excessive rotor overspeed or droop during maneuvers, which is corrected by revising the engine / fuel control system.

All these reference studies demonstrate that the dynamic coupling of engine with fuel control and rpm-governor units is a critical aspect for turbine powered helicopter. As a matter of fact, the coupled rotor / engine / fuel control system dynamics is dominated by responses in two frequency ranges: a low frequency mode of operation that characterizes the fastness of the engine speed response to fuel control inputs, and the higher frequency modes associated with the torsional dynamics of the drive train coupled with blade lag motion. Therefore, the design of modern helicopter engine / fuel control systems is based on both the maximization of the responsiveness of the low frequency mode and the stabilization of the higher frequency drive system dynamics. Unfortunately, the need for high control system gains, that enhance the quickness of helicopter engine response, may compromise the stability of the drive system torsional modes.

A discussion of engine control compensation for power turbine speed governing system stabilization is presented in Ref. [7]. The results demonstrate that the notch-filter concept, applicable to all advanced helicopter systems incorporating electronic power turbine speed control, may produce excellent transient response characteristics while maintaining good stability margins.

The development of new advanced engine control strategies for micro-processor based fuel control systems on a twin engine helicopter is discussed in Ref. [12]. Some of these concepts are classically adaptive in that the control modifies itself online to deal with engine deterioration, surge or failure. Different specific applications were investigated such as lower fuel consumption, the reduction of deadman's region and torsional stability with inoperative rotor blade lag dampers. This last problem is solved by incorporating second order notch filtering in the fuel control power turbine governor. The damping of the rotor drive train was artificially increased by phasing higher frequency fuel flow inputs such that the resulting engine torque opposes drive train oscillations. It was also demonstrated that handling qualities can be improved in maneuvering flight including rotor speed information into the control.

An integrated flight and propulsion control scheme for the UH-60 helicopter, based on a LQR governor, is evaluated in Ref. [15] and it is found to be superior to the basic control in most areas. An active control strategy is suggested for enhancing drive train stability in Ref. [20]

A parallel research activity in the field of mathematical modeling was developed, with the aim of extending the accuracy of simulations, that may assess the impact of engine/drive train dynamics on the operational effectiveness of the aircraft.

A partial derivatives engine model based on generalized factors [2] was used by Sanders [3] to simulate the torque response to fuel inputs. Equations were developed for the torsional motion of a gas turbine engine geared to a helicopter rotor in which the blades were hinged to the shaft. The rotor-engine system was represented by two rotating masses connected by a torsional spring. Comparison of the system response calculated from these equations with the experimentally observed frequency response showed satisfactory agreement. The resonant frequency and damping were accurately represented, but the amplitude response above resonance was underestimated.

The torsional stability of a closed-loop dynamic system (a typical transport helicopter speed governor, gas turbine engine and drive train) is evaluated in Ref. [8]. The inclusion of a nonlinear mechanical coupling was found to be effective in stabilizing the previously unstable helicopter drive system. This was explained observing that the shaft damping was artificially increased by means of an elastomeric damper and the rotor inertia of the helicopter drive system was isolated from the engine inertia.

A flight dynamics simulation tool (Genhel) has been developed in Ref. [9] which treats engine, fuel control, rotor and airframe. This nonlinear mathematical model is adopted in Ref. [10] to investigate the torsional compatibility of the engine / fuel control with helicopter rotor and airframe dynamics, at frequencies below the rotational speed. The authors conclude that without application of full dynamic system flight simulation, advanced electronic fuel controls may become unnecessarily constrained in order to minimize risk or, if unconstrained, may introduce a new set of dynamic problems. Some analytical results presented show the promising potential of using body state feedback to the fuel control to enhance aircraft handling qualities (particularly in the yaw degree of freedom) and rotor droop characteristics.

A simple model, which consists of two masses with a centrifugal spring, assuming a very stiff rotor shaft, is proposed in Ref. [16]. Dynamic interactions between rotor, propulsion system and drive train are analyzed for a hover flight case for both hingeless and articulated rotor. The results of eigenvalue analysis and time simulations demonstrate that the rotor speed degree of freedom couples only with the collective lag mode. The effects of bandwidth and delay for the engine fuel control are discussed.

A high order mathematical model of a helicopter (UM-Genhel) that includes the complete dynamics of the aircraft, including the rotor, inflow and propulsion system dynamics is described in Ref. [17]. The mathematical model of the propulsion system is presented in Ref. [16]. The effect of drive train torsional dynamics is not included. The influence of the propulsion system dynamics is assessed by comparing frequency responses of flight test data and of a full order model against frequency responses of a linearized model with the dynamics of the propulsion system removed. The dynamics of the propulsion system affects very little the predictions of the pitch and roll rate frequency responses. The most significant effects of the propulsion system is observed in the vertical acceleration and yaw rate responses for frequencies between 0.1 and 1 rad/s.

An alternative approach to the problem of modeling the effects of propulsion system dynamics on handling qualities is proposed in Ref. [18]. Drive train torsional dynamics is described by discrete masses and a flexible rotor shaft. This simplified formulation is extremely general and it was found to be accurate for the estimation of the dominant first torsional mode, which is the most important for the integration of engine and airframe. The stability of an integrated flight and propulsion control scheme, including rotor states feedback, is also discussed.

A blade element model for a hingeless helicopter was developed in Ref [29]. The results confirm that, although the inclusion in the model of drive train degrees of freedom promotes intermodal couplings, pitch and roll short term handling qualities are largely unaffected by propulsion system design.

A complete engine / governor / drive train model was integrated into the DLR helicopter simulation code SIMH [21]. For this purpose, the main rotor formulation comprising rigid lead/lag and flap degrees of freedom is resolved for rotor speed and drive train dynamics. Parameterized engine and governor models are evaluated from complex high order physical descriptions, using reduction schemes, while still being physical meaningful, allowing for application in real time conditions. The parameters of the reduced lower order models were optimized by comparing the simulation results with BO105 flight test data in hover and forward flight. With the inclusion of both engine and drive train dynamics, improvement in the dynamic prediction of helicopter shaft torque, rotor speed, heave and yaw motion for collective and pedal inputs could be achieved.

The analysis of references on mathematical modeling shows that engine manufactures tend to use a sophisticated engine dynamic model in conjunction with a rather rudimentary model of helicopter rotor / airframe dynamics when designing the control system. High fidelity models for engine dynamics are accurate but the computational workload is generally high. Another critical aspect is the different time scaling of the two sets of differential equations, governing the engine and the airframe response. Furthermore, these nonlinear computer simulations become inadequate for the analysis of helicopter handling qualities requirements when an extremely simplified model of rotor / airframe dynamics is adopted. Some simulations are based on a linearized state space representation of the response of the specific propulsion system [19]. Nevertheless, a high order validated model of the propulsion system is always necessary and the extension to different engine/drive train configurations is not straightforward.

On the other hand, helicopter manufacturers have traditionally used the opposite approach. As a result, the dynamic interface problems that are not anticipated in the design stage can appear later in the flight test phase of a helicopter development program, requiring modifications to fix the problems [13].

Therefore, a balance between the two different levels of accuracy is required in order to obtain a comprehensive mathematical model able to represent the influence of fuel control and drive train/propulsion system design parameters on helicopter handling qualities.

Present Work

The objectives of this paper are:

1. To include the formulation developed in Ref. [18] in a high order mathematical model of articulated rotor and helicopter airframe, and to validate the dynamic response for a realistic helicopter configuration

2. To analyze the effects of governor and drive train design parameters on rotorcraft stability in hovering flight, considering two different mathematical models: a high order blade element type model (34 DOFs) and a reduced order analytical model (8 DOFs)

3. To evaluate the impact of rpm-governor design parameters on the application of some relevant ADS-33D handling qualities criteria, by means of simulations performed with the higher order mathematical model (34 DOFs).

Mathematical Model

The mathematical model developed is a nonlinear blade-element type representation of a single rotor helicopter with rigid fuselage (see Fig. 1).
The analysis of short term response to control inputs in coordinated turns presented in Ref. [29, 30] was

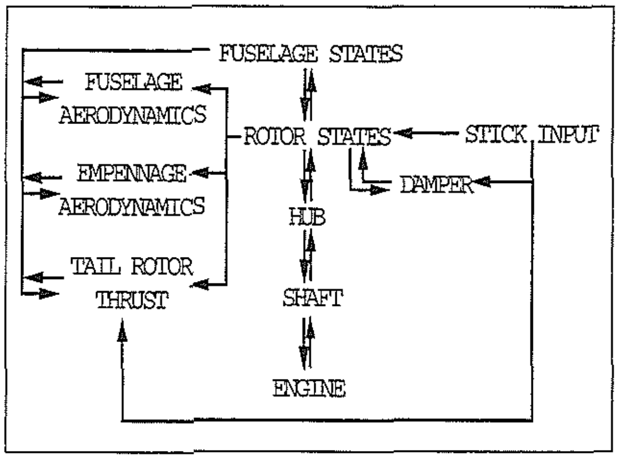

Figure 1: The flight dynamics simulation model.

based on a previous model implementation for a different helicopter, that was later extended for validation purposes.

The main rotor blades are individually modeled as rigid bodies and the coupled flap-lag dynamics is included. The equations of motion of the rotor are formulated and solved in a rotating coordinate system.

No small angle assumption is invoked for aerodynamic angles of rotor and fuselage. The profile aerodynamic loads are calculated using two dimensional blade element theory with table lookup for blade twist and lift/drag coefficients.

The reactions generated by the lag dampers are nonlinear functions of the axial velocity of the damper itself [9, 26].

The aerodynamics of fuselage and stabilizers is modeled using coefficients derived from wind tunnel data.

A three-state dynamic inflow model [23] is used for the main rotor.

The rigid body motion of the aircraft is modeled using six nonlinear force and moment equations and three kinematic relations (Euler equations).

The forces (X,Y,Z) and the moments (L,M,N) depend on the blade motion and provide the main source of coupling between the rotor and the fuselage. They also contain contributions from fuselage, tail rotor and other aerodynamic surfaces. Both dynamic and aerodynamic rotor-fuselage couplings are included in the model. The latter type of coupling is typically due to the interaction of the rotor wake with the fuselage and tail surfaces, and to the changes of rotor inflow due to the presence of the fuselage.
The most important feature of the set of equations of motion for the fuselage used in the present study is

that the fuselage states need not to be small quantities; thus, all the kinematic nonlinearities associated with the motion of the fuselage are retained.

The propulsion system model is a slightly modified version of that used by Chen [18], consisting of discrete masses and a flexible rotor shaft.
The equation for engine/drive train torque equilibrium is:

$$I_{eq}\ddot{\psi}_1 + B_1 r_g^2 \dot{\psi}_1 + K_S(\psi_1 - \psi_b) = r_g Q_E$$

where, as in Ref. [18], B_1 is the engine damping, I_{eq} is the moment of inertia of the propulsion system, referred to the rotor speed, K_S is the torsional stiffness of the rotor shaft, Q_E is the engine torque, and r_g is the engine to rotor nominal rpm ratio. The equation for shaft equilibrium is:

$$I_{hub}\ddot{\psi}_b - K_S(\psi_1 - \psi_b) = \sum_{k=1}^{n_b} e \cdot R_{2k}$$

where I_{hub} is the moment of inertia of the hub. This formulation is slightly more general than that of Ref. [18], which focused on specific rotor modes in which the blades moved in lag only, and with identical angular displacements. The forcing torque is obtained by summing the force contributions R_{2k} of each blade in the hub plane and perpendicular to the root segment of the blade, multiplied by the hinge offset moment arm e.

The order of the complete system is 34 and the state vector $\mathbf{x}$ can be represented as:

$$\mathbf{x} = \begin{Bmatrix} \mathbf{x_F} \\ \mathbf{x_R} \\ \dot{\mathbf{x}}_\mathbf{R} \\ \mathbf{x_I} \\ \mathbf{x_E} \end{Bmatrix}$$

The vector $\mathbf{x_F}$ contains the fuselage degrees of freedom and is defined as

$$\mathbf{x_F} = [u\, v\, w\, p\, q\, r\, \theta\, \phi\, \psi]^T$$

The vectors $\mathbf{x_R}$ and $\mathbf{x_I}$ include the rotor and inflow degrees of freedom, transformed in a body-fixed reference system:

$$\mathbf{x_R} = [\beta_o\, \beta_{1c}\, \beta_{1s}\, \beta_{N/2}\, \zeta_o\, \zeta_{1c}\, \zeta_{1s}\, \zeta_{N/2}]^T$$

$$\mathbf{x_I} = [\lambda_o\, \lambda_s\, \lambda_c]^T$$

Finally, the vector $\mathbf{x_E}$ refers to the engine and drive train states:

$$\mathbf{x_E} = [Q_E w_f \psi_1\, \Omega_1\, \psi_b\, \Omega]^T$$

where $\Omega = \dot{\psi}_b$ and $\Omega_1 = \dot{\psi}_1$.
The control vector $\mathbf{u}$ is defined as:

$$\mathbf{u} = [\theta_o\, \theta_{1s}\, \theta_{1c}\, \theta_{TR}\, \dot{\theta}_o\, \dot{\theta}_{1s}\, \dot{\theta}_{1c}\, \dot{\theta}_{TR}]^T$$

The presence of time derivatives in $\mathbf{u}$ is required for a correct modeling of the lag dampers.

The effect of the primary pitch control actuators is also included in the mathematical model and their dynamic response is represented by a second order transfer function [26].

The trim procedure is the same as in [25, 22]. Thus, the rotor equations of motion are transformed into a system of nonlinear algebraic equations using a Galerkin method (10 eqns.). The algebraic equations enforcing force and moment equilibrium (9 eqns.), the additional kinematic equations (2 eqns.) that must be satisfied in forward flight (or in a turn), and the momentum inflow equations for both main and tail rotor (3+1 eqns.) are added to the rotor equations, and the combined system (25 eqns.) is solved simultaneously. The solution yields the harmonics of a Fourier series expansion of the rotor degrees of freedom, the pitch control settings, trim attitudes and rates of the entire helicopter, and main and tail rotor inflow.
Flight without sideslip is arbitrarily assumed for $\mu \leq 0.1$, while roll attitude is set to zero for higher airspeed.
The propulsion system is not included in the trim process. This implies two assumptions. The first is that the engine can generate a sufficient torque in any flight condition. The second is that the small fluctuations of rotor speed associated with the lag dynamics of the rotor do not affect the engine torque.

A linearized set of small perturbation equations can be extracted from the nonlinear model:

$$\dot{\mathbf{x}} = [A] \cdot \mathbf{x} + [B] \cdot \mathbf{u}$$

The coefficients of the model are derived numerically about the trim condition, using finite difference approximations. The linearization of the rotor equations is carried out in the rotating coordinate system. A multiblade coordinate transformation (i.e. a modal coordinate transformation that is limited to the rotor degrees of freedom) converts the linearized state matrices to a fixed frame [24, 26]. This transformation only partially reduces the periodicity of the system.

Therefore, an averaging of the linearized coefficients evaluated at several positions along the blade azimuth is required.

The response to pilot inputs is obtained from direct numerical integration of the equations of motion. Note that the program is designed for off-line simulation only. The procedure preserves the full periodicity of the helicopter response (Ref. [27]). This is confirmed by the time histories of the thrust coefficient C_T and the vertical acceleration presented in Fig. 2. The integration is performed starting from a trim condition keeping all the controls fixed. The time response is given by the superposition of a steady state (the trim initial condition) and a small n_b/rev oscillation.

The time responses to fuel flow inputs and rpm-governor dynamics (PID control) are reproduced with a simplified approach based on the model presented in Ref. [28]:

$$\begin{aligned} \dot{Q}_E &= T_Q \Delta Q_E + T_{wf} w_f + K_C T_{wf} \Delta\theta_o \\ \tau_{wf}\dot{w}_f &= -\Delta w_f + K_D \dot{\Omega} + K_P \Delta\Omega + K_I \int \Delta\Omega \end{aligned}$$

The present mathematical model was selected in order to include one time scale only.

Results

The configuration adopted for the numerical simulations is similar to the medium size tactical utility helicopter described in Ref. [9]. This aircraft is a single rotor helicopter (Tab. 1) with articulated flap and lag hinges. The flight condition corresponds to an altitude of 5250 ft in standard atmosphere ($C_T/\sigma \approx 0.081$). The stability augmentation and flightpath stabilization are disabled. The stabilator positions are held fixed at trim setting determined by the numerical computations presented in Ref. [17].

Rotor speed	27 rad/s
Rotor disc radius	8.177 m
Blade m.a.c.	0.527 m
Rotor hinge offset e	0.381 m / 4.66 %
Blade Lock number γ	7.783
n_b	4
Gross weight	71196 N
CG station / waterline	8.915 m / 5.880 m
K_S	541065 Nm/rad
I_{eq}	1673 Kgm^2
I_{hub}	164 Kgm^2
B_1	0 Nm s
r_g	76
K_D	0 Kg s
K_P	-0.05397 Kg
K_I	-0.08246 Kg/s
K_C	0.052 Kg/s
τ_{wf}	0.067 s
T_Q	-7.847 s^{-1}
T_{wf}	61100 Nm/kg

Table 1: The helicopter configuration.

Model Validation

System eigenvalues were identified by comparing frequencies and eigenvectors. Propulsion system dynamics enhances intermodal couplings that complicate the identification of poles and normal modes. The related eigenvectors include the engine variables (ψ_b, ψ_1) and their time derivatives. Merging of the fuselage modes is also observed in some flight conditions. Additional modes are introduced in the complete dynamic system [18]:

- first torsional mode : this is primarily an engine / shaft motion coupled with blade lag dynamics;
- second torsional mode : the hub motion is coupled with blade lag dynamics;

The natural frequency of the first torsional mode is quite accurately predicted by the model. The torsional resonance for the real aircraft [15] occurs at $\omega_n \approx 17$ rad/s. The first torsional mode is originated by the migration of two lead lag complex conjugate roots, and these eigenvalues migrate back to $\omega_L = \sqrt{(k_\zeta + eM_\zeta\Omega_0^2)/I_\zeta} = 7.222$ rad/s increasing both K_S and I_{eq} (Tab. 2).

	without governor		with governor	
engine param.	ξ (-)	ω_n (rad/s)	ξ (-)	ω_n (rad/s)
$K_S = K_{S_0}$ $I_{eq} = I_{eq_0}$	0.227	17.509	0.160	16.591
$K_S \to \infty$ $I_{eq} \to \infty$	0.452	6.930	0.452	6.946

Table 2: The first torsional mode in hover.

The time response to collective and fuel flow step was also analyzed (Fig. 3). The rpm response is characterized by a sharp deceleration of the engine/drive train system for positive collective step.

The oscillatory behavior of Ω and Ω_1 during the initial transient of the rpm response demonstrates that the first torsional mode is excited by the command input. The time history of vertical acceleration is substantially different when engine/drive train dynamics is included. The flattened response for vertical acceleration predicted by the varying rpm model with rpm-governor is confirmed by flight test data [18]. It is also evident that the constant rotational speed model overpredicts the heave response in the first transient phase. The opposite is verified in the second part of the time history. Differently, when the rpm-governor is disabled, the inclusion of propulsion system dynamics produces a significant reduction of the steady state rate of climb in hover related to the sharp deceleration of the main rotor angular speed Ω.

Time domain response to collective input ($\dot{\Omega} \neq 0$, $K_P = K_{P_0}$ and $K_I = K_{I_0}$) is also compared in Fig. 4 with dissimilar flight tests performed on a hovering UH-60A helicopter [28]. The rpm and the fuel flow response were obtained so that the torque overshoot was the same of flight test data. The rpm variation is quite well reproduced by TPI simulations, although a marginal discrepancy for initial fuel flow response modeling is observed (also confirmed by the validations presented in Ref. [28]).

Stability Analysis

Two different mathematical models are considered for the stability analysis of the first torsional mode: a high order blade element type model and a reduced order analytical model (the relevant equations are provided in the Appendix). A comparison of open loop time response to step fuel flow input for the complete (34 DOFs) and the reduced model (8 DOFs) is shown in Fig. 5. This comparison demonstrates that short term response (shaft torsion and blade lag) is quite accurately predicted by the low order analytical model.

The effect of shaft stiffness K_S is presented in Fig. 6. The rpm-governor is here disabled ($K_P = K_I = 0$). The increase of stiffness K_S promotes a remarkable non linear increase of natural frequency and damping ratio. The presence of the lag dampers (that were not included in Ref. [18]) promotes the coupling between flap and lag/shaft modes for the higher order model. This result cannot be reproduced by the reduced order model, where lag dampers are supposed to be decoupled from flap motion and flap dynamics is neglected.

The effect of rpm-governor proportional gain K_P in hovering flight is examined in Fig. 7. The coupling between fuel flow / torque dynamics and drive train is enhanced for higher feedback gains, where the stability of the first torsional mode is compromised. The response to collective input is analyzed with the higher order simulation model in Fig. 8. Flap and lag oscillations occur when the gain K_P exceeds the stability limit of the first torsional mode.

The unstable behavior is also accurately predicted by the reduced order model and it can be assumed that this last model is able to reproduce the stability degradation due to the increase of fuel flow proportional gain K_P. Hence, a complete analysis of the controller stability boundaries for the first torsional mode was performed assuming that both shaft stiffness K_S and equivalent inertia I_{eq} could be varied within a specified range. This result is presented in Fig. 9 in which the equivalent inertia is normalized with respect to the rotor inertia I_R and the torsional stiffness K_S is converted into the equivalent degrees of static torsion $\psi_1 - \psi_b = \frac{\tau_g Q_E}{K_S}$. The dimensions and the weight of the rotor are held constant. The diagram shows that K_S is the most effective parameter for extending the boundary for acceptable gains K_P within the realistic range of the inertial ratio I_R/I_{eq}.

Furthermore, the decrease of the fuel flow time constant τ_{wf} promotes the reduction of the dynamic stability limit $(K_P)_{\xi=0}$. This result is also confirmed in Fig. 10 where the effects of the parameters K_P and τ_{wf} on torsional dynamics are analyzed. The damping ξ is increased for higher delays while the natural frequency ω_n of the first torsional mode remains fairly constant within the stable range of rpm-governor design parameters.

Handling Qualities

Finally, the analysis of the impact of rpm-governor design parameters on some relevant ADS-33D handling qualities criteria is considered. The requirements concerning rotor rpm governing in Ref. [1] recommend that the rotational regime of the main rotor should remain within specified limits. Apart from this very general considerations, the effect of rpm-governor is apparently not considered, assuming that a degradation of drive train stability should probably compromise the general aircraft handling qualities. A review of the application of the principal criteria for the reference helicopter configuration is here performed in order to verify if any relationship may exist between torsional oscillations and handling qualities criteria.

Simulations performed with the higher order model show that drive train and rpm-governor design have a limited effect on short term longitudinal and lateral handling qualities (see also Ref. [29]). Short term directional handling qualities also remain fairly constant when governor design parameters are modified within a realistic range. Anyway, remind that the model does not include the torsional flexibility of tail rotor transmission.

Heave response is obviously influenced by rpm-governor design and the most effective parameter is the proportional gain K_P. The effect of K_P on flight path control handling qualities is presented in Fig. 11. Mixing of stick inputs is enabled. The criterion described in Ref. [1] is based on the assumption that the height rate response to a collective step input should have a qualitative first order shape. The increase of rpm-governor proportional gain within the stable range ($K_P < (K_P)_{\xi=0}$) promotes a reduction of time delay. Differently, exceeding $(K_P)_{\xi=0}$ does not seem to be substantially beneficial. The time constant $T_{\dot{h}} = -1/Z_W$ is marginally affected by the design of the rpm-governor. An evident change for vertical damping is only observed for open loop response ($K_P = K_I = 0$).

The criterion for interaxis coupling, i.e. yaw rate response due to collective step input, is presented in Fig. 11. Higher HQ levels are observed for higher feedback gains K_P and the results are apparently unaffected by drive train torsional instability.

The torque response to collective input is analyzed in Fig. 11. The increase of feedback gain promotes a shift of HQ from marginal Level 2 to Level 1 and most of the decrease of time to first torque peak is observed for $K_P < (K_P)_{\xi=0}$. An excess of feedback (i.e. promoting drive train instability) gives a negligible advantage in terms of torque response.

Concluding Remarks

1. The formulation developed in Ref. [18] was included in a high order mathematical model of articulated rotor and helicopter airframe, and the dynamic response was validated for a realistic helicopter configuration.

2. The effects of governor and drive train design parameters on rotorcraft stability in hovering flight were analyzed, considering two different mathematical models: a high order blade element type model (34 DOFs) and a reduced order analytical model (8 DOFs). This last simplified model was found to be accurate for predicting drive train torsional stability.

3. The impact of rpm-governor design parameters on the application of some relevant ADS-33D handling qualities criteria was evaluated. Handling qualities criteria does not reflect the stability degradation of drive train due to high closed loop gains, as it is assumed that torsional oscillations should remain within acceptable limits. Only heave response parameters are substantially affected by governor design, and apparently no specific advantage derives from excessive feedback in terms of flight path control and torque response.

Appendix
The Reduced Order Analytical Model

In order to derive a low order approximation for the drive train torsional dynamics, the basic equations obtained in Ref. [18] are reduced to a first order form and linearized at the reference equilibrium condition ($\Omega = \Omega_1 = \Omega_0$, $\dot{\zeta} = 0$ and $\zeta = \zeta_0$).
The two additional equations presented in Ref. [28] related to the effects of torque and rpm-governor dynamics are also included. Therefore, the reduced order system has 8 degrees of freedom with the following state-space representation $\dot{\mathrm{x}} = [\mathbf{A}] \cdot \mathrm{x}$, and the nonzero elements of the state matrix $\mathbf{A}$ are:

$$a_{12} = 1 \qquad a_{21} = \frac{I_\zeta K_S}{d} \qquad a_{23} = \frac{-I_\zeta K_S}{d}$$

$$a_{25} = \frac{ac}{d} \qquad a_{26} = \frac{-ac_\zeta}{d} \qquad a_{34} = 1$$

$$a_{41} = \frac{K_S}{I_{eq}} \qquad a_{43} = \frac{-K_S}{I_{eq}} \qquad a_{44} = \frac{-B_1 r_g^2}{I_{eq}}$$

$$a_{47} = \frac{r_g}{I_{eq}} \qquad a_{56} = 1 \qquad a_{61} = \frac{-bK_S}{d}$$

$$a_{63} = \frac{bK_S}{d} \qquad a_{65} = \frac{-cI_R}{d} \qquad a_{66} = \frac{c_\zeta I_R}{d}$$

$$a_{77} = T_Q \qquad a_{78} = T_{wf} \qquad a_{81} = \frac{e}{d\tau_{wf}}$$

$$a_{82} = \frac{K_P}{\tau_{wf}} \qquad a_{83} = \frac{-f}{d\tau_{wf}} \qquad a_{85} = \frac{acK_D}{d\tau_{wf}}$$

$$a_{86} = \frac{-ac_\zeta K_D}{d\tau_{wf}} \qquad a_{88} = \frac{-1}{\tau_{wf}}$$

where

$$x = [\int \Delta\Omega \, \Delta\Omega \int \Delta\Omega_1 \, \Delta\Omega_1 \, \Delta\zeta \, \dot{\zeta} \, \Delta Q_E \, \Delta w_f]^T$$

and

$$\begin{aligned}
a &= -n_b \cdot (I_\zeta + eM_\zeta) \\
b &= -(I_\zeta + eM_\zeta) \\
c &= -(eM_\zeta \Omega_0^2 + k_\zeta) \\
d &= ab - I_R I_\zeta \\
e &= f + K_I d \\
f &= I_\zeta K_S K_D \\
I_R &= I_{hub} + n_b \cdot (I_\zeta + 2eM_\zeta + m_\zeta e^2)
\end{aligned}$$

The model is derived neglecting the effects of blade aerodynamics and assuming that the damper lag reaction ΔQ_ζ on the generic blade can be linearized ($\Delta Q_\zeta = c_\zeta \cdot \dot{\zeta} + k_\zeta \cdot \Delta\zeta$). For the reference helicopter the lag damper damping ratio is $\zeta_D = c_\zeta / 2\sqrt{(k_\zeta + eM_\zeta \Omega_0^2) I_\zeta} \approx 0.396$.

References

[1] "Aeronautical Design Standard ADS - 33D Handling Qualities Requirements for Military Rotorcraft", U. S. Army Aviation and Troop Command, St. Louis, MO, July 1994

[2] Ketchum, J. R., Craig, R. T., "Simulation of Linearized Dynamics of Gas-Turbine Engines", NACA-TN-2826, 1952

[3] Sanders, J.C., "Influence of Rotor Engine Torsional Oscillation on Control of Gas Turbine Geared to a Helicopter Rotor", NACA-TN-3027, 1953

[4] Kelley, H.L., Pegg, R.J., Champine, R.A., "Flying Quality Factors Currently Limiting Helicopter Nap-of-Earth Maneuverability as Identified by Flight Investigation", NASA-TN-D-4931, 1968

[5] Corliss, L. D., "Effects of Engine and Height Control Characteristics on Helicopter Handling Qualities", J. of the American Helicopter Society, vol. 28, July 1983

[6] Fredrickson, C., Rumford, K., Stephenson, C., "Factors Affecting Fuel Control Stability of a Turbine Engine/Helicopter Rotor Drive System", J. of the American Helicopter Society, vol. 16, Jan. 1972

[7] Alwang, J.R., Skarvan, C.A., "Engine Control Stabilizing Compensation Testing and Optimization", J. of the American Helicopter Society, vol. 22, n. 3, 1977

[8] Darlow, M.S., Vance, J.M., "Torsional Stability Analysis of a Gas Turbine Powered Helicopter Drive System", ASME Gas Turbine Conference, Zurich, Switzerland, 1974

[9] Howlett, J.J., "UH-60A Black Hawk Engineering Simulation Program: Volume I - Mathematical Model", NASA-CR-166309, Dec. 1981

[10] Kuczynski, W.A., Twomey, W.J., Howlett, J.J., "The Influence of Engine/Fuel Control Design on Helicopter Dynamics and Handling Qualities", 35th AHS Annual Forum, Washington D.C., USA, 1979

[11] Warmbrodt, W., Hull, R., "Development of a Helicopter Rotor/Propulsion System Dynamics Analysis", AIAA/SAE/ASME 18th Joint Propulsion Conference, Cleveland, USA, 1982

[12] Howlett, J.J., Morrison, T., Zagranski, R.D., "Adaptive Fuel Control for Helicopter Applications", J. of the American Helicopter Society, vol. 29, n. 4, 1984

[13] Chen, R.T.N., Mihaloew, J. R., "Rotorcraft Flight Propulsion Control Integration", Vertiflite, vol. 30, n. 6, 1984

[14] Johnson,W., "Recent Developments in the Dynamics of Advanced Rotor Systems ", AGARD LS-139, n. 4, 1985

[15] Mihaloew, J. R., Ballin, M. G., Ruttledge, D. C. G., "Rotorcraft Flight Propulsion Control Integration: an Eclectic Design Concept", NASA-TP-2815, 1988

[16] Ockier, C.J., "Engine-Rotor Interaction: a Dynamic Analysis in Hover", MS Thesis, University of Maryland, 1990

[17] Kim, F.D., "Formulation and Validation of High Order Mathematical Models of Helicopter Dynamics", PhD Dissertation, Univ. of Maryland, 1991

[18] Chen, R.T.N., "An Exploratory Investigation of the Flight Dynamic Effects of Rotor RPM Variations and Rotor State Feedback in Hover", NASA-TM-103968, 1992

[19] Duyar, A., Gu, Z., Litt, J.S., "A Simplified Dynamic Model of the T700 Turboshaft Engine", J. of the American Helicopter Society, vol. 40, n. 3, 1995

[20] Krysinski, T., "Active Control of Aeromechanical Stability", AGARD Symposium on Advances in Rotorcraft Technology, Ottawa, Canada, 1996

[21] Hamers, M., von Grunhagen, W., "Dynamic Engine Model Integrated in Helicopter Simulation", 23rd European Rotorcraft Forum, paper n. 91, Dresden, 1997

[22] Chen, R.T.N., and Jeske, J.A., "Kinematic Properties of the Helicopter in Coordinated Turns", NASA-TP-1773, 1981

[23] Peters, D.A., HaQuang, N., "Dynamic Inflow for Practical Applications", J. of the American Helicopter Society, vol. 33, n. 4, 1988

[24] Johnson, W., "Helicopter Theory ", Dover Publications, 1994, pp. 349-361

[25] Celi, R., "Hingeless Rotor Dynamics in Coordinated Turns", J. of the American Helicopter Society, vol. 36, n. 4, 1991

[26] Kim, F.D., Celi, R., Tischler, M.B., "High-Order State Space Simulation Models of Helicopter Flight Mechanics", J. of the American Helicopter Society, vol. 38, n. 4, 1993

[27] Kim, F.D., Celi, R., Tischler, M.B., "Forward Flight Trim and Frequency Response Validation of a Helicopter Simulation Model", J. of Aircraft, vol. 30, n. 6, 1993

[28] Fletcher, J.W., "A Model Structure for Identification of Linear Models of the UH-60 Helicopter in Hover", NASA-TM-110362, 1995

[29] Guglieri, G., Celi, R., Quagliotti, F.B., "Effect of Propulsion System Dynamics on Rotorcraft Aeromechanical Stability in Straight and Turning Flight", AGARD Symposium on Advances in Rotorcraft Technology, Ottawa, Canada, 1996

[30] Guglieri, G., Celi, R., "On Some Aspects of Helicopter Flight Dynamics in Steady Turns", J. of Guidance, Control and Dynamics, vol. 21, n. 2, 1998

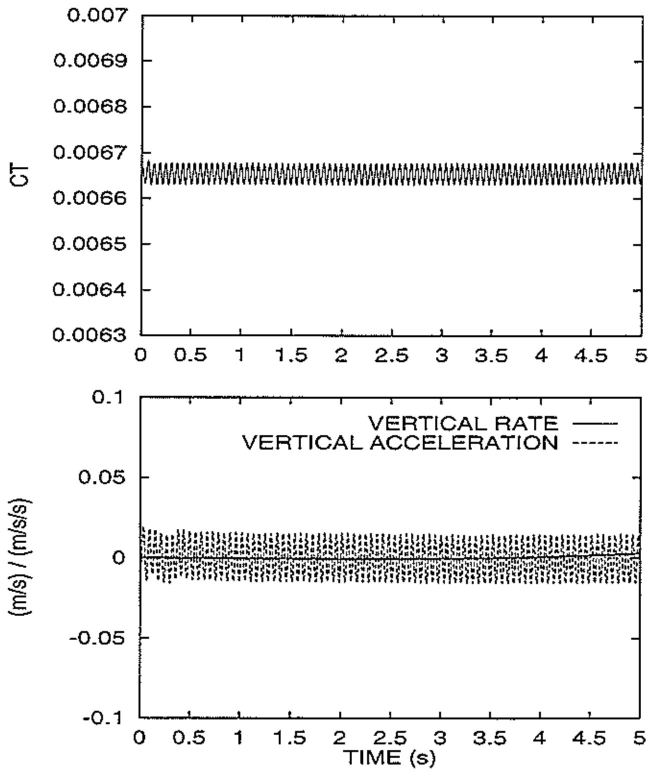

Figure 2: Time history of C_T and vertical acceleration ($\mu = 0.2$).

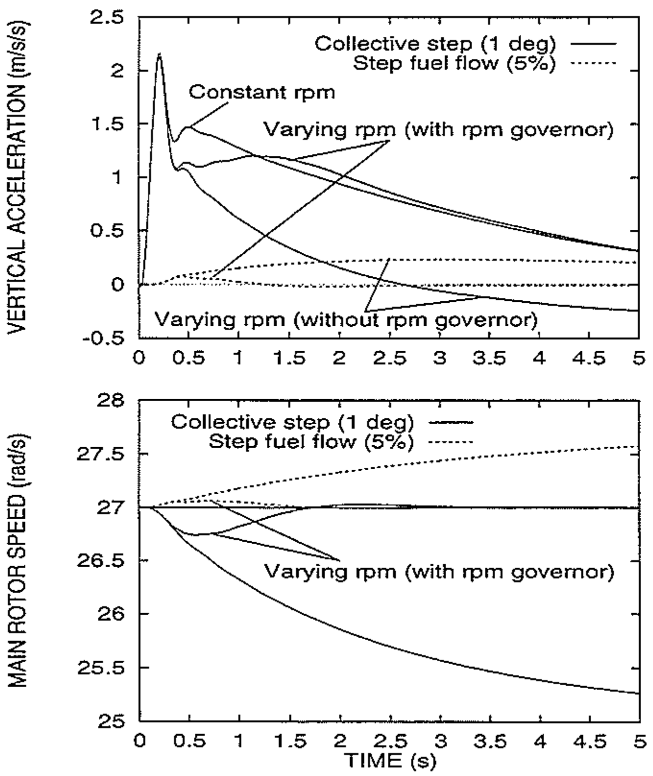

Figure 3: Vertical acceleration and rpm response to collective step and fuel flow input in hover.

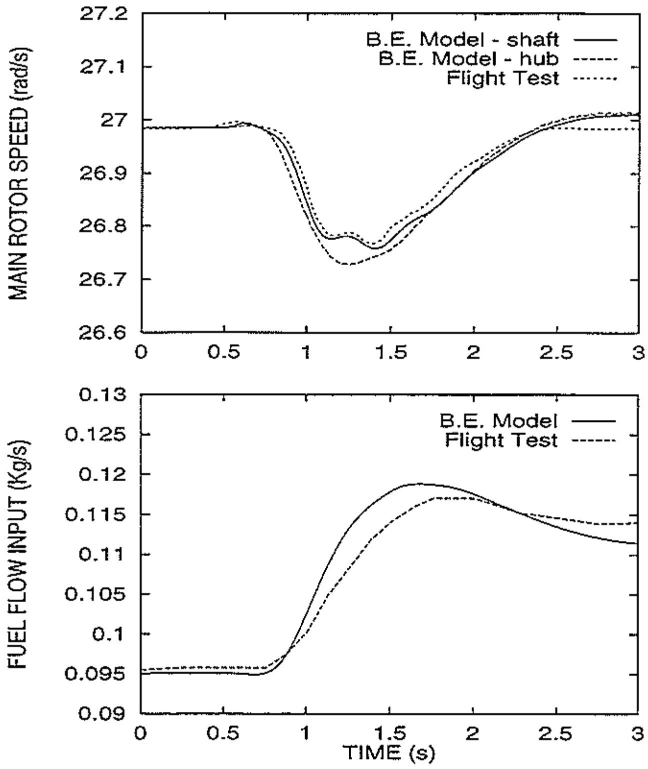

Figure 4: Response to collective step input in hover: comparison with flight test data.

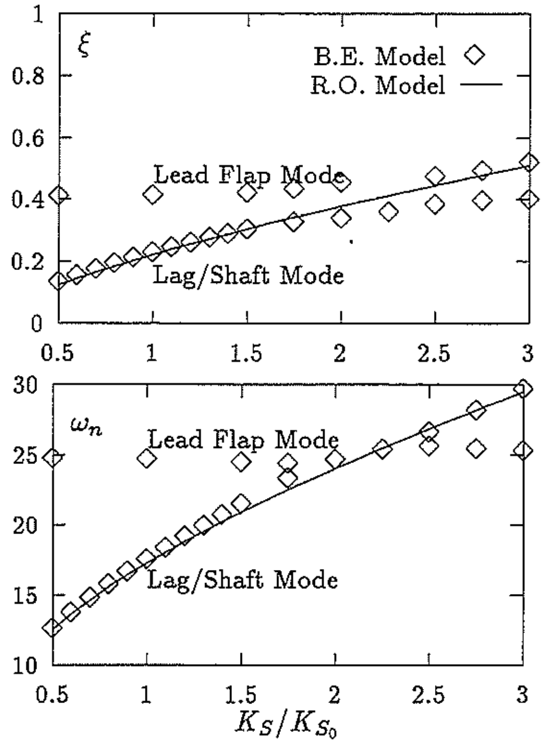

Figure 6: The effect of shaft stiffness K_S on the first torsional mode in hover.

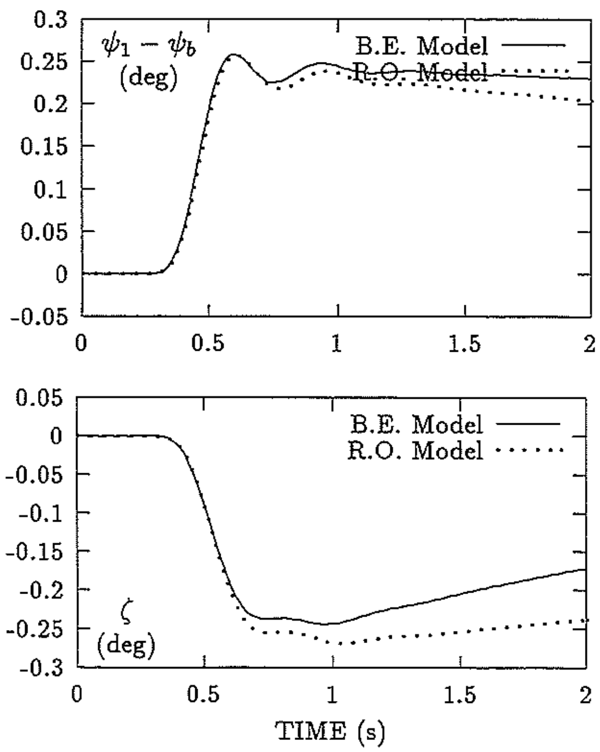

Figure 5: Comparison of short term open loop response to a step fuel flow input (5%) in hover.

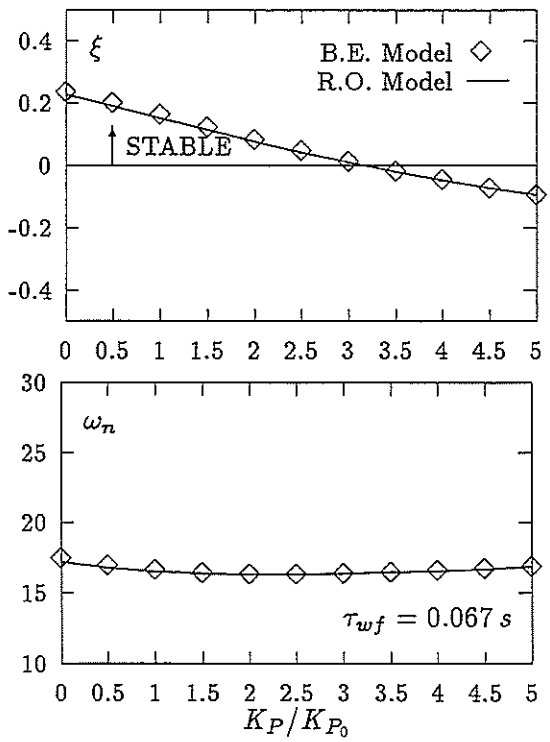

Figure 7: The effect of fuel controller gain on the stability of the first torsional mode in hover.

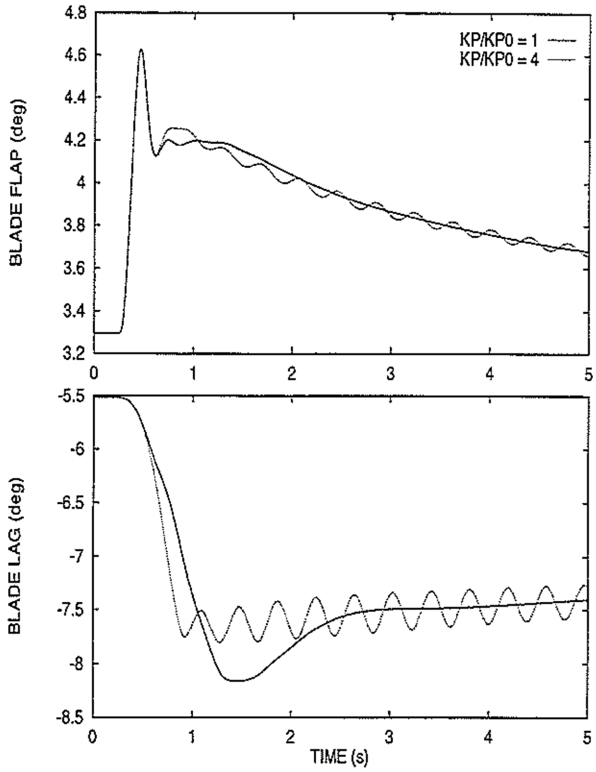

Figure 8: The effect of proportional gain on the response to collective input (1.6 deg) in hover.

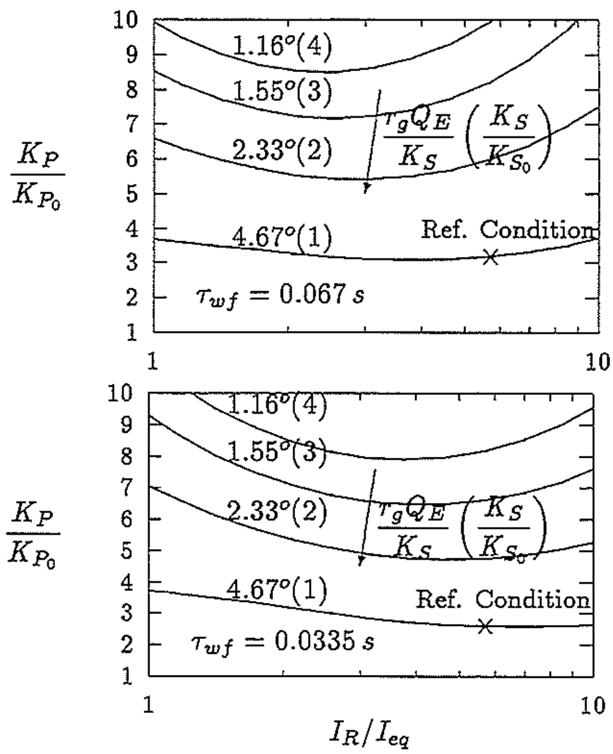

Figure 9: The stability limit for the fuel controller proportional gain K_P in hover.

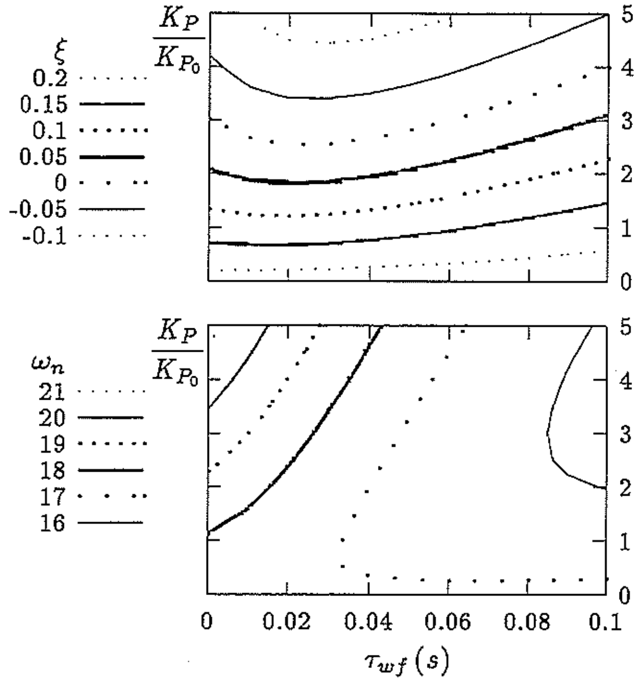

Figure 10: The effect of fuel controller gain K_P and delay τ_{wf} on the first torsional mode in hover.

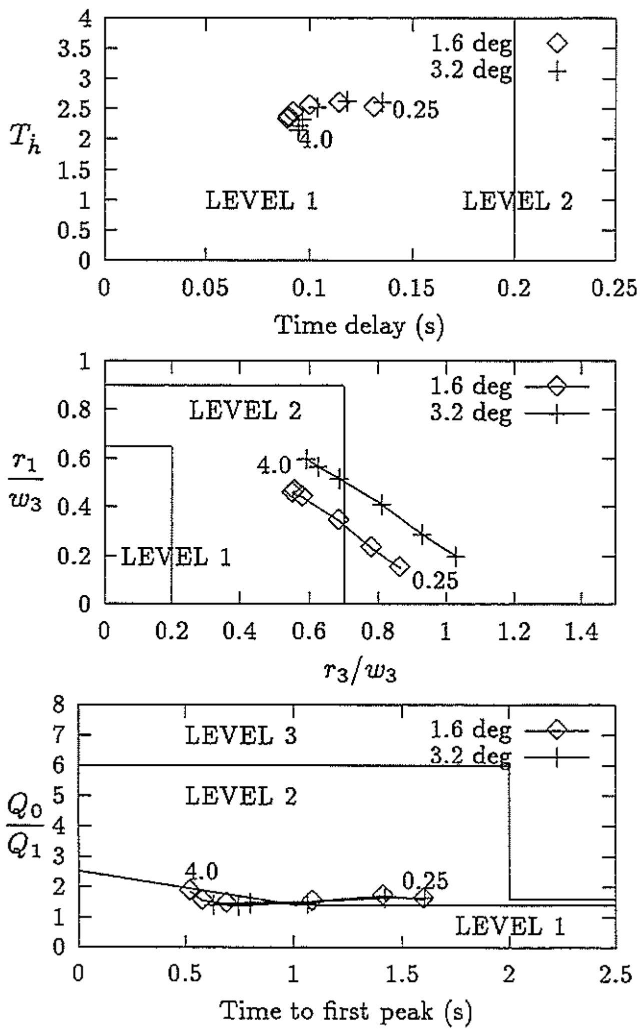

Figure 11: The effect of K_P/K_{P_0} on heave response.